ISSN: 2639-7455

Research Article

Earth & Environmental Science Research & Reviews

Monitoring The Land Surface Temperature and Its Correlation with NDVI of Chiniot by Using GIS Technology and Remote Sensing

Ahmed Yaseen Ghouri*, Aleeza Khan, Fahad Rasheed

University of Gujrat Hafiz Hayat Campus Jalalpur Road Gujrat, Pakistan

***Corresponding author**

Ahmed Yaseen Ghouri, University of Gujrat Hafiz Hayat Campus Jalalpur Road Gujrat, Pakistan.

Submitted: 11 Apr 2022; **Accepted:** 19 Apr 2022; **Published:** 26 Apr 2022

Citation: *Ahmed Yaseen Ghouri, Aleeza Khan, Fahad Rasheed. (2022). Monitoring The Land Surface Temperature and Its Correlation with NDVI of Chiniot by Using GIS Technology and Remote Sensing. Eart & Envi Scie Res & Rev. 5(2):01-09.*

Abstract

The unplanned and rapid increased in unban area have changed the atmospheric conditions and the non-urban area have less warm as compare to urban areas. In study area little portion of Chenab River include and the river bed contains the sand it shows high temperature value due to its specific heat energy. For this study Lands at-5 (February2000), Landsat-7(February 2005,2010) and Landsat-8 (Feb2015, Feb2020, Feb2022) Data acquired from USGS. The LST and NDVI correlation is negative and it is clearly seen that in the analysis of Landsat-8 (OLI/TIRS) the Land Surface Temperature is increases 3.5408° C from 2015 to 2022. The analysis of Landsat-7(ETM+) the Land Surface Temperature is increases 3.3461° C from 2005 to 2010. In the Correlation analysis(LST&NDVI) the most of vegetation occurs between 11 °C to 28 °C.

Keywords: GIS, Remote Sensing, LST, NDVI, Landsat-8, Climate Change, Correlation

Introduction

The Land Surface Temperature (LST) is that the radiative skin temperature of the land surface, as measured within the direction of the remote device [1]. It's likely from Top-of-Atmosphere brightness temperatures from the infrared spectral channels of a constellation of fixed satellites [2]. Its estimation additional depends on the ratio, the vegetation covers and also the soil wet. LST may be a mixture of vegetation and bare soil temperatures [3]. as a result of each respond apace to changes in incoming radiation thanks to implementers and aerosol load modifications and variation of illumination, the LST displays fast variations too [4]. In turn, the LST influences the partition of energy between ground and vegetation, and determines the surface air temperature [5].

Over the past many decades in Remote Sensing community, land surface temperature (LST) is found to be one among the foremost necessary parameters within the physical processes of surface energy and water balance at native through world scales [6]. LST estimation provides information concerning temporal and spacial variations of the surface equilibrium state and is of basic importance in several applications [7]. LST is getting used in an exceedingly type of areas like evapotranspiration, climate change, hydrological cycle, vegetation watching, urban climate and environmental studies, among others [8]. Since the launch of the Landsat-8 satellite (also referred to as Landsat knowledge Continuity Mission, LDCM) in Feb 2013 continuity of remote sensing knowledge at high spacial resolution nonheritable by instruments on board previous [9]. Landsat satellites like the multispectral scanner system (MSS), the thematic mapper (TM), and therefore the increased thematic plotter and (ETM+) [10].

Normalized distinction Vegetation Index (NDVI) quantifies vegetation by measurement the distinction between near-infrared (which vegetation powerfully reflects) and red light (which vegetation absorbs) [11]. NDVI continually ranges from -1 to +1. however, there isn't a definite boundary for every kind of land cover. for instance, after you have negative values, it's extremely seemingly that it's water [12]. On the opposite hand, if you've got associate NDVI worth on the brink of +1, there's a high chance that it's dense inexperienced leaves. however, once NDVI is on the brink of zero, there aren't inexperienced leaves associated it may even be an urbanized space [13]. The result of this formula generates a value between -1 and +1. If you have low reflectance (or low values) in the red channel and high reflectance in the NIR channel, this will yield a high NDVI value [14]. And vice versa. Overall, NDVI is a standardized way to measure healthy vegetation. When you have high NDVI values, you have healthier vegetation. When you have low NDVI, you have less or no vegetation [15].

Landsat 5 carried the same instruments, including the Thematic Mapper and Multi-Spectral Scanner [16]. The Multi-Spectral Scanner was powered down in 1995, but reactivated again in 2012 (Muttitanon & Tripathi, 2005) [17]. Landsat 7 has a solid-state memory of 378 G bits (roughly 100 images) [18]. The main instrument on board Landsat 7 is the Enhanced Thematic Mapper Plus (ETM+), a whisk broom scanner image sensor Landsat 8 is an American Earth observation satellite launched on 11 February 2013 [19]. It is the eighth satellite in the Landsat program; the seventh to reach orbit successfully. Originally called the Landsat Data Continuity Mission (LDCM), it is a collaboration between NASA and the United States Geological Survey (USGS) [20]. NASA Goddard Space Flight Center in Greenbelt, Maryland, provided development, mission systems engineering, and acquisition of the launch vehicle while the USGS provided for development of the ground systems and will conduct on-going mission operations [21, 22]. It comprises the camera of the Operational Land Imager (OLI) and the Thermal Infrared Sensor (TIRS) which can be used to study Earth surface temperature and is used to study global warming [23]. The satellite was built by Orbital Sciences Corporation, who served as prime contractor for the mission [24]. The spacecraft's instruments were constructed by Ball Aerospace & Technologies and NASA's Goddard Space Flight Center (GSFC), and its launch was contracted to United Launch Alliance (ULA) [25]. During the first 108 days in orbit, LDCM underwent checkout and verification by NASA and on 30 May 2013 operations were transferred from NASA to the USGS when LDCM was officially renamed to Landsat 8 [26].

Study Area

Chiniot is that the thirty sixth district of Punjab province Pakistan Located on the bank of the river Chenab, it is the 28th largest city of Pakistan. it's given the standing of district in 2009 (Raza & Mehmood, 2014). Major a part of the district consists upon the agricultural areas and their basic supply of financial gain is agriculture. The folks of villages square measure un-educated and have lack of awareness. Chiniot comprises AN collection of many tiny villages and cities. Villages square measure commonly "Chak No" whereas Chiniot town contains of redundant Municipal Committee (MC) Chiniot. Out of total 44 Union Councils (UC) within the Chiniot district, eight Urban UC area unit comprised in Chiniot town. Chiniot town had a population of 251,671 in 1998, that accumulated up to 314,917 in 2017, The population in chinoit for 2021 is 222,525. In the last national census of Asian country and it's being expected that population of Chiniot can become 0.4 million in 2030 (PMSIP, 2009). Chiniot is located within the Northwest of canal Chenab. it's coupled with the most cities of Punjab, like city, Faisalabad, Sargodha and Jhang via roads. It is 160 km distant from city to the east, concerning thirty km from metropolis to south-west, concerning 56 km from Sargodha to the west and 86 km from Jhang to south-west. Chiniot is found at latitude of 31°43′ to 31°44′ North latitude and 72°58′ to 73°0′ East great circle on the world [27, 28]. (as shown figure 1)

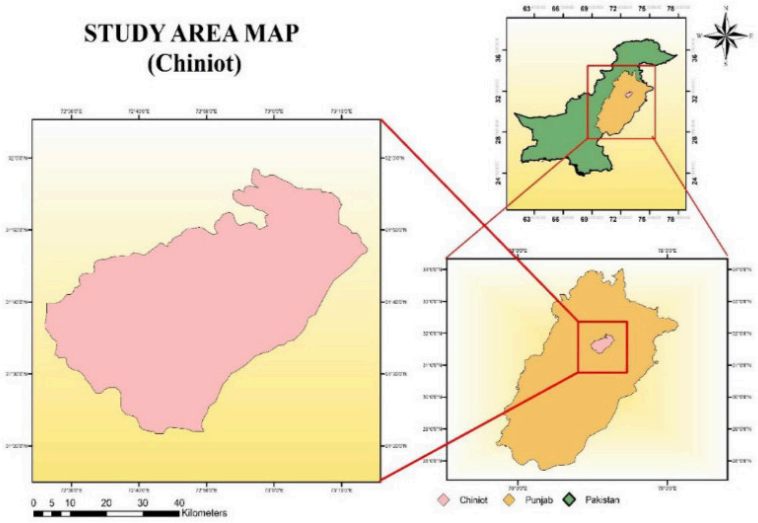

Figure 1: Study Area Map (Chiniot)

Methodology

NDVI

NDVI is used to quantify vegetation greenness and vegetation density as well as plant health. NDVI is calculated as a ratio between the red (R) and near infrared (NIR) values. Download the data from the USGS, then import the raster image into the ArcMap. Open the ArcMap toolbox called spatial analysis tool open it then select map algebra then open the raster calculator, here we can write the mathematical equation: (NIR - R) / (NIR + R).

For LandSat-7&5: Band4 subtract form Band3 and then divide it with Band 4 Add Band 3

Mathematical equation;
NDVI = (Band 4 – Band 3) / (Band 4 + Band 3).

For LandSat-8 Band 5 subtract form Band4 and then divide it with Band 5 Add Band 4

Mathematical equation;
NDVI = (Band 5 – Band 4) / (Band 5 + Band 4)

Land surface temperature (LST) of Landsat 5& 7

First download the Landsat-7 image from USGS then import the thermal band (Band 6 is the thermal band in the Landsat-7) in ArcMap. Then Convert the Digital Number (DN's) into the radiance by using the following equation;

Radiance can be computed by using this formula
$L\lambda = ML \times Qcal + AL$

Surface temperature was computed from the Top of Atmosphere radiance image using the formula,

$T = K2 / In (K1 / L\lambda + 1)$

Similarly, for Landsat TM, TOA radiance in Wm-2Sr-1, was computed using the formula,

$L\lambda = (Lmax\lambda – Lmin\lambda) / QCALmax – QCALmin \times (DN – QCALmin) + Lmin\lambda$

While the surface temperature from the computed radiance is given by

$T = K2 / In(K1 / L\lambda + 1)$

The computed temperature in Kelvin scale was converted to Celsius scale using the relationship,

$C = T – 273.15$

Where,
L =Spectral radiance
QCAL = Quantized calibrated pixel value in DN
LMAX= Spectral radiance scaled to QCALMAX in (Watts/(m2 • sr • µm))

LMIN= Spectral radiance scaled to QCALMIN in (Watts/(m2 • sr • µm))

QCALMIN = Minimum quantized calibrated pixel value (corresponding to LMINA) QCALMAX = Maximum quantized calibrated pixel value (corresponding to LMAX,) in

DN= 225

Where,

T= Effective at-satellite temperature in Kelvin
K2 = Calibration constant 2
K1 = Calibration constant 1
*Spectral radiance in (Watts/(m^2 * sr * µm))*

Table 1

SENSOR	CONSTANT 1 - KT (WATTS/(M2 * SR * UM))	CONSTANT 2 - K2 KELVIN
LANDSAT-7 ETM+	666.09	1282.71
LANSAT -5 TM	607.76	1260.56

Land surface temperature (LST) of Landsat 8

The Land Surface Temperature is calculated by the Landsat 08 thermal bands (band 10 and band 11). we applied a group of equations through a raster image calculator in ArcMap.

Calculation of Top of Atmospheric (TOA) spectral radiance
The top of Atmosphere can be calculated by using the following formula

TOA (L) = ML * Qcal + AL

The vales of M_L and A_L is got from the MLT file.

Where;
M_L = Band-specific multiplicative rescaling factor from the metadata
Q_{cal} = corresponds to band 10 and band 11
A_L = Band-specific additive rescaling factor from the metadata.

TOA to Brightness Temperature conversion

BT = (K2 / (ln (K1 / L) + 1)) - 273.15

K_1 = Band-specific thermal conversion (constant
K_2 = Band-specific thermal conversion (constant)
L = Top of Atmosphere
Calculate the mean of band 10 and band 11 BT by using a tool called Cell Statistics. (calcalute mean value).

Calculate the NDVI

NDVI = (Band 5 – Band 4) / (Band 5 + Band 4)

calculation of the NDVI is important because, subsequently, the proportion of vegetation (P_v), which is highly related to the NDVI, and emissivity (ε), which is related to the P_v, must be calculated. Calculate the proportion of vegetation Pv:

Pv = Square ((NDVI – NDVImin) / (NDVImax – NDVImin))

Calculate Emissivity ε

The value of 0.986 corresponds to a correction value of the equation.
ε = 0.004 * Pv + 0.986

Calculate the Land Surface Temperature

Apply the LST equation to obtain the surface temperature Map.

$$LST = (BT / (1 + (w * BT / p) * Ln(\varepsilon)))$$

Correlation LST & NDVI

Add the image into ArcMap who NDVI and LST is calculated, then apply the tool (Create fishnet). Create Fishnet is completely run then use the tool (Extract Multi Values to point) on both images (LST & NDVI) then clip tool is used on the output which generates in the result of Extract Multi Values to point. Open the attribute table of clip image here two new fields are created one is NDVI other one is LST. Go to Create Graph option select scatter plot, on x-axis assign LST and on y-axis assign NDVI click on next. Finally, Correlation graph of LST & NDVI is created.

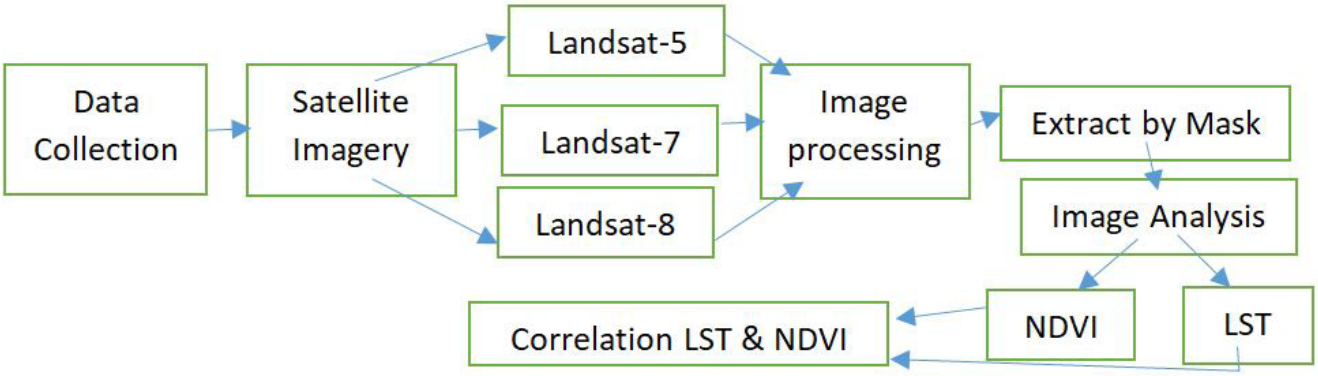

Result

NDVI

The result of NDVI of February 2000 shows the maximum values is 0.04186 and the minimum value is -0.0666. The result of second Image of NDVI (funerary 2005) shows the maximum values is 0.5882 and the minimum value is -0.0769. The result of third image of NDVI (February 2010) shows the maximum value is 0.7108 while the minimum value is -0.1184. The result of fourth image of NDVI (February 2015) shows the maximum value is 0.4839 and the minimum value -0.1313. The result of fifth image of NDVI (February 2020) shows the maximum value is 0.5024 and the minimum value -0.1467. The result of sixth image of NDVI (February 2022) shows the maximum value is 0.5393 and the minimum value -0.1375. Day by day built-up Area is increases and the area for crop production and green space decreases. The area of snow, barren land, sand shows the very low NDVI values (For example 0.1 or less) in the maps its clear see the area around the river and built-up there is no vegetation its value is less than 0.1. Sparse vegetation (senescing crops, grasslands, shrubs) it shows the NDVI from 0.2 to 0.5. High value of NDVI is 0.6 to 0.9 in the forest region or when the crops at peak growth stage. In February 2010 the crops are at peak growth stage shows the 0.7108. The Climate is also change in February 2010 the crops is at their peak growth stage while in 2022 the crops show the moderate value i.e. 0.5393 (as shown in fig 2.1, 2.2, 2.3, 2.4, 2.5, 2.6)

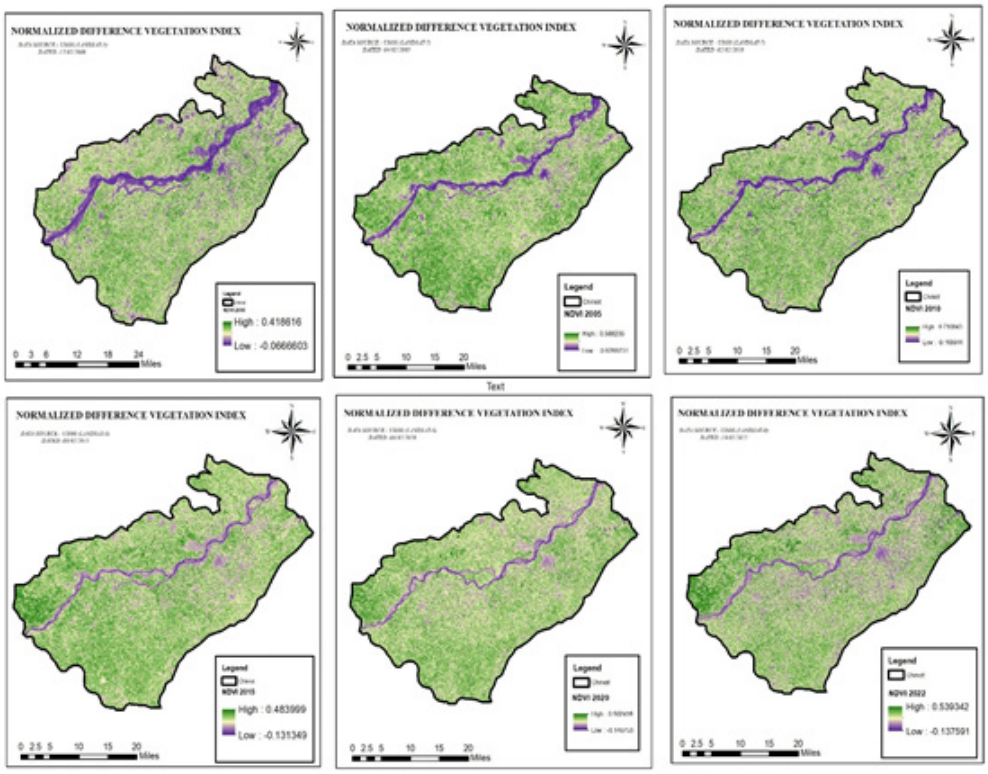

Figure 2.1, 2.2, 2.3, 2.4, 2.5, 2.6

Land Surface Temperature

The first analysis of (Landsat-5) February 2000 shows the maximum high land surface temperature is 34.0663oC and the minimum land surface temperature detect by the sensors are 10.4435°C. The second Analysis of February 2005 (Landsat-7) shows the maximum high land surface temperature is 31.1872 °C and the minimum land surface temperature is 9.8375 °C. The third Analysis of February 2010 (Landsat-7) shows the maximum high temperature is 34.5333 °C and minimum land surface temperature is 11.594 °C. The change in land surface temperature from February 2000 to February 2005 is 2.8758 °C (decrease) and the change in land surface temperature from February 2005 to February 2010 is 3.3461°C (increase as shown in figure 3.1, 3.2, 3.3).

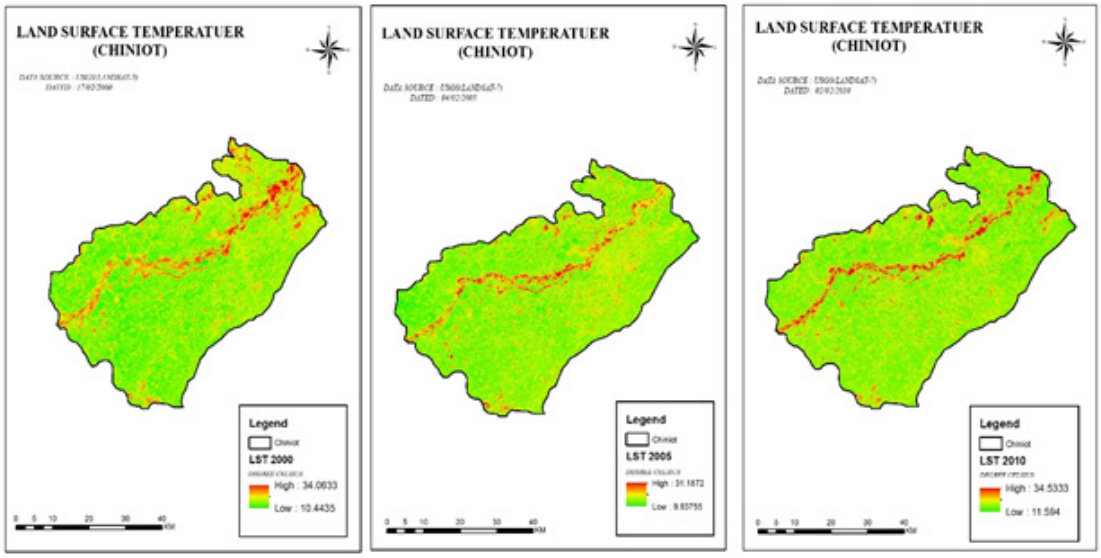

Figure 3.1, 3.2, 3.3

The fourth analysis of (Landsat-8) February 2015 shows the maximum high land surface temperature is 31.4826°C and the minimum land surface temperature detect by the sensors are 15.1603°C. The fifth analysis of (Landsat-8) February 2020 shows the maximum high land surface temperature is 32.0681°C and the minimum land surface temperature detect by the sensors are 8.1522°C. The sixth analysis of (Landsat-8) February 2022 shows the maximum high land surface temperature is 35.0234°C and the minimum land surface temperature detect by the sensors are 9.5734°C. The change in land surface temperature from February 2015 to February 2020 is 0.5855°C (increase) and the change in land surface temperature from February 2020 to February 2022 is 2.9553°C (increase). as shown in fig 4.1, 4.2, 4.3.

The red line indicates high temperature value there is actually river bed made-up of sand. As sand absorb maximum heat due to specific heat energy (the amount of energy needed to rise the temperature of an object) in this case sand receiving its energy from the sun. Sand has very low specific heat energy as compare to water, so sand get rapidly warm from sunlight and rapidly cool in the absence of sunlight. (as shown in fig 4.1, 4.2, 4.3).

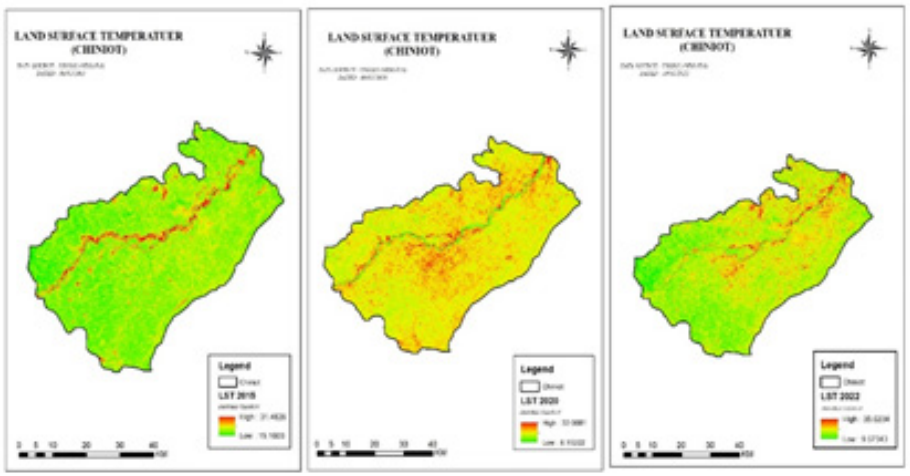

Figure 4.1, 4.2, 4.3

On y-axis temperature show in degree Celsius while on x-axis shows the date of satellite image on which the LST analysis is perform. It is clearly seen that the LST increases.

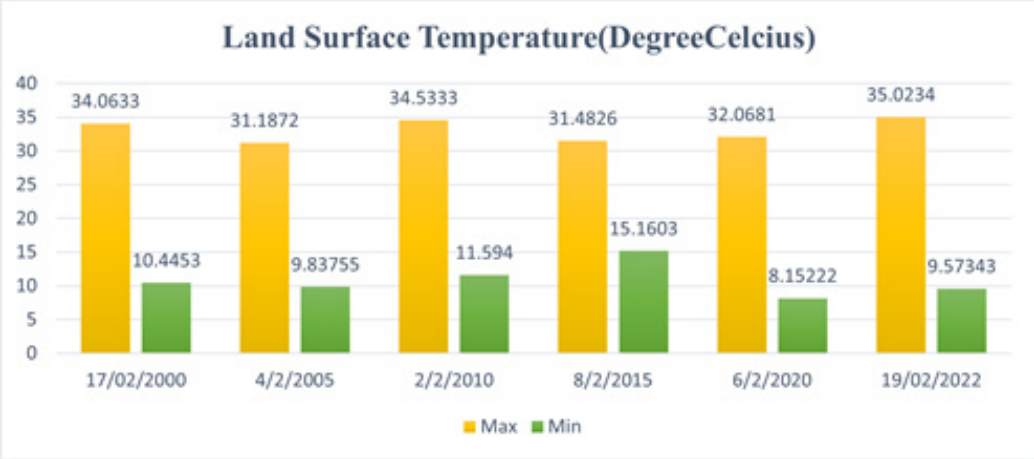

Figure 5

Correlations of Land Surface Temperature and Normalized Difference Vegetation Index

The Analysis of Landsat-5(TM) February 2000 the correlation of land surface temperature and normalized difference vegetation index show the trend between 11.529°C to 18.24°C. The Analysis of Landsat-7 (ETM+) February 2005 the correlation of land surface temperature and normalized difference vegetation index show the trend between 21.532 to 26.21°C. The Analysis of Landsat-7(ETM+) February 2010 the correlation of land surface temperature and normalized difference vegetation index show the trend between 21.642°C to 29.027°C (as shown in fig 6.1, 6.2, 6.3).

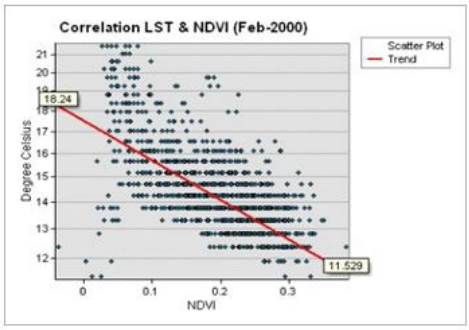

Figure 6.1

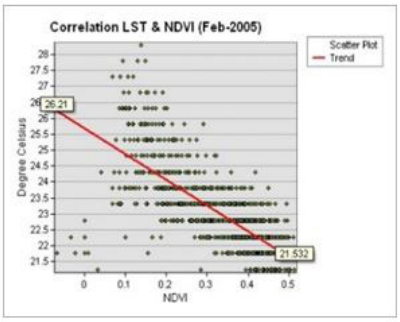

Figure 6.2

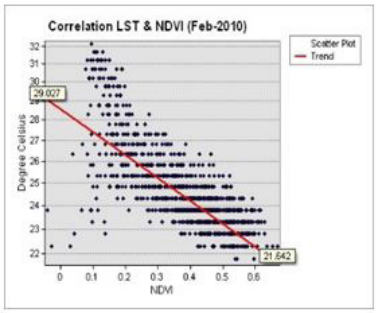

Figure 6.3

The Analysis of Landsat-8(OLI/TIRS) February 2015 the correlation of land surface temperature and normalized difference vegetation index show the trend between 15.982°C to 20.506°C. The Analysis of Landsat-8(OLI/TIRS) February 2020 the correlation of land surface temperature and normalized difference vegetation index show the trend between 16.089°C to 17.649°C. The Analysis of Landsat-8(OLI/TIRS) February 2022 the correlation of land surface temperature and normalized difference vegetation index show the trend between 18.201°C to 12.307°C. It indicates that the most of vegetation occurs where the land surface temperature between 11°C to 27°C (as shown in fig 7.1, 7.2, 7.3).

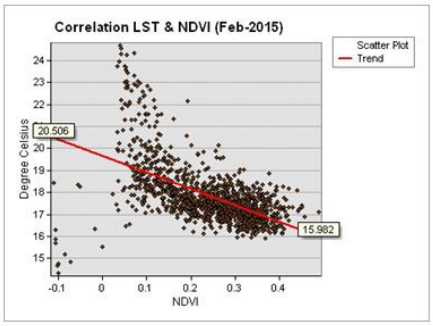

Figure 7.1

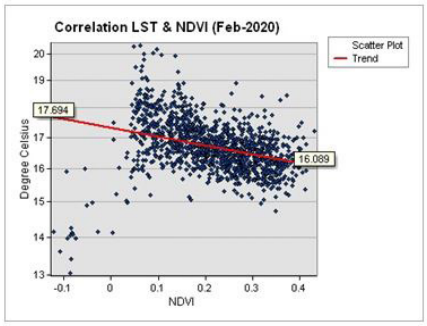

Figure 7.2

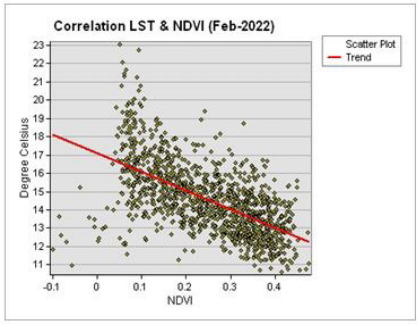

Figure 7.3

Table 2

DATA SOURCE & DATAED		LAND SURFACE TEMPERATURE		NORMALIZED DIFFERENCE VEGETATION INDEX	
DATA SOURCE	DATE	MAX	MIN	MAX	MIN
LANDSAT-5	17/02/2000	34.0633	10.4453	0.4186	-0.0666
LANDSAT-7	04/2/2005	31.1872	9.83755	0.5882	-0.0769
LANDSAT-7	02/2/2010	34.5333	11.594	0.7108	-0.1184
LANDSAT-8	08/2/2015	31.4826	15.1603	0.4839	-0.1313
LANDSAT-8	06/2/2020	32.0681	8.15222	0.5024	-0.1467
LANDSAT-8	19/02/2022	35.0234	9.57343	0.5393	-0.1375

Conclusion & Discussion

Land surface temperature is an important variable with in the earth climate system. The land surface temperature increases due to change in climate Change and urban sprawl. In this study Landsat5, Landsat 7 & Landsat-8 data is acquired from United States Geological Survey (USGS). The urban area shows the high values of LST as compare to vegetation area. The analysis of Landsat-7 (ETM+) show that the Land Surface Temperature is increases 3.3461oC from 2005 to 2010. In February 2010 the crops are at peak growth stage shows the 0.710 (NDVI) while in 2022 the crops show the moderate value i.e. 0.5393 (NDVI) The analysis of Landsat-8 (OLI/TIRS) the Land Surface Temperature is increases 3.5408oC from 2015 to 2022. The changed and unchanged bare land and built-up area suffer from the increasing trend of land surface temperature and it significantly present the influence in the climate change.

References

1. Horiuchi, Y., Chino, A., Matsuo, Y., Kishihara, T., Uragami, N., Fujimoto, Y., ... & Igarashi, M. (2013). Diagnosis of laterally spreading tumors (LST) in the rectum and selection of treatment: characteristics of each of the subclassifications of LST in the rectum. Digestive Endoscopy, 25(6), 608-614.
2. Aslan, N. A. G. İ. H. A. N., & Koc-San, D. İ. L. E. K. (2016). ANALYSIS OF RELATIONSHIP BETWEEN URBAN HEAT ISLAND EFFECT AND LAND USE/COVER TYPE USING LANDSAT 7 ETM+ AND LANDSAT 8 OLI IMAGES. International Archives of the Photogrammetry, Remote Sensing & Spatial Information Sciences, 41.
3. Neteler, M. (2010). Estimating daily land surface temperatures in mountainous environments by reconstructed MODIS LST data. Remote sensing, 2(1), 333-351.
4. Hasanlou, M., & Mostofi, N. (2015, June). Investigating urban heat island estimation and relation between various land cover indices in Tehran city using Landsat 8 imagery. In Proceedings of the 1st International Electronic Conference on Remote Sensing, Basel, Switzerland (pp. 1-11).
5. Sun, D., & Kafatos, M. (2007). Note on the NDVI-LST relationship and the use of temperature-related drought indices over North America. Geophysical Research Letters, 34(24).
6. Zhou, X., Yan, N., Chuang, K. T., & Luo, J. (2014). Progress in La-doped SrTiO 3 (LST)-based anode materials for solid oxide fuel cells. Rsc Advances, 4(1), 118-131.
7. Li, H., Sun, D., Yu, Y., Wang, H., Liu, Y., Liu, Q., ... & Cao, B. (2014). Evaluation of the VIIRS and MODIS LST products in an arid area of Northwest China. Remote Sensing of Environment, 142, 111-121.
8. Benali, A., Carvalho, A. C., Nunes, J. P., Carvalhais, N., & Santos, A. (2012). Estimating air surface temperature in Portugal using MODIS LST data. Remote Sensing of Environment, 124, 108-121.
9. Deo, R. C., & Şahin, M. (2017). Forecasting long-term global solar radiation with an ANN algorithm coupled with satellite-derived (MODIS) land surface temperature (LST) for regional locations in Queensland. Renewable and Sustainable Energy Reviews, 72, 828-848.
10. Mostovoy, G. V., King, R. L., Reddy, K. R., Kakani, V. G., & Filippova, M. G. (2006). Statistical estimation of daily maximum and minimum air temperatures from MODIS LST data over the state of Mississippi. GIScience & Remote Sensing, 43(1), 78-110.
11. Pettorelli, N., Vik, J. O., Mysterud, A., Gaillard, J. M., Tucker, C. J., & Stenseth, N. C. (2005). Using the satellite-derived NDVI to assess ecological responses to environmental change. Trends in ecology & evolution, 20(9), 503-510.
12. Chen, J., Jönsson, P., Tamura, M., Gu, Z., Matsushita, B., & Eklundh, L. (2004). A simple method for reconstructing a high-quality NDVI time-series data set based on the Savitzky–Golay filter. Remote sensing of Environment, 91(3-4), 332-344.
13. Carlson, T. N., & Ripley, D. A. (1997). On the relation between NDVI, fractional vegetation cover, and leaf area index. Remote sensing of Environment, 62(3), 241-252.
14. Gamon, J. A., Field, C. B., Goulden, M. L., Griffin, K. L., Hartley, A. E., Joel, G., ... & Valentini, R. (1995). Relationships between NDVI, canopy structure, and photosynthesis in three Californian vegetation types. Ecological Applications, 5(1), 28-41.
15. Wang, J., Rich, P. M., & Price, K. P. (2003). Temporal responses of NDVI to precipitation and temperature in the central Great Plains, USA. International journal of remote sensing, 24(11), 2345-2364.
16. Chander, G., & Markham, B. (2003). Revised Landsat-5 TM radiometric calibration procedures and postcalibration dynamic ranges. IEEE Transactions on geoscience and remote sensing, 41(11), 2674-2677.
17. Muttitanon, W., & Tripathi, N. K. (2005). Land use/land cover changes in the coastal zone of Ban Don Bay, Thailand using Landsat 5 TM data. International Journal of Remote Sensing, 26(11), 2311-2323.
18. Roy, D. P., Kovalskyy, V., Zhang, H. K., Vermote, E. F., Yan, L., Kumar, S. S., & Egorov, A. (2016). Characterization of Landsat-7 to Landsat-8 reflective wavelength and normalized difference vegetation index continuity. Remote sensing of Environment, 185, 57-70.
19. Markham, B., Storey, J., & Morfitt, R. (2015). Landsat-8 sensor characterization and calibration. Remote Sensing, 7(3), 2279-2282.
20. Tollefson, J. (2013). Landsat 8 to the rescue: NASA prepares to launch satellite that will continue historic record of global change. Nature, 494(7435), 13-15.
21. Rajeshwari, A., & Mani, N. D. (2014). Estimation of land surface temperature of Dindigul district using Landsat 8 data. International Journal of Research in Engineering and Technology, 3(5), 122-126.
22. Roy, D. P., Wulder, M. A., Loveland, T. R., Woodcock, C. E., Allen, R. G., Anderson, M. C., ... & Zhu, Z. (2014). Landsat-8: Science and product vision for terrestrial global change research. Remote sensing of Environment, 145, 154-172.
23. Claverie, M., Masek, J. G., Ju, J., & Dungan, J. L. (2017).

Harmonized landsat-8 sentinel-2 (HLS) product user's guide. National Aeronautics and Space Administration (NASA): Washington, DC, USA.
24. Loveland, T. R., & Irons, J. R. (2016). Landsat 8: The plans, the reality, and the legacy. Remote Sensing of Environment, 185, 1-6.
25. Adiri, Z., Lhissou, R., El Harti, A., Jellouli, A., & Chakouri, M. (2020). Recent advances in the use of public domain satellite imagery for mineral exploration: A review of Landsat-8 and Sentinel-2 applications. Ore Geology Reviews, 117, 103332.
26. Skakun, S., Wevers, J., Brockmann, C., Doxani, G., Aleksandrov, M., Batič, M., ... & Žust, L. (2022). Cloud Mask Intercomparison eXercise (CMIX): An evaluation of cloud masking algorithms for Landsat 8 and Sentinel-2. Remote Sensing of Environment, 274, 112990.
27. Carlson, T. N., & Ripley, D. A. (1997). On the relation between NDVI, fractional vegetation cover, and leaf area index. Remote sensing of Environment, 62(3), 241-252.
28. Wang, J., Rich, P. M., & Price, K. P. (2003). Temporal responses of NDVI to precipitation and temperature in the central Great Plains, USA. International journal of remote sensing, 24(11), 2345-2364.